

Na, Al, AND O ABUNDANCES OF OPEN CLUSTERS NGC 7142, NGC 6939, AND IC 4756

HEATHER R. JACOBSON

Department of Astronomy, Indiana University, Bloomington, IN 47405, USA; hrj@astro.indiana.edu

EILEEN D. FRIEL¹

Division of Astronomical Sciences, National Science Foundation, Arlington, VA 22230, USA; efriel@nsf.gov

AND

CATHERINE A. PILACHOWSKI

Department of Astronomy, Indiana University, Bloomington, IN 47405, USA; catyp@astro.indiana.edu

Received 2007 May 23; accepted 2007 June 11

ABSTRACT

We present an analysis of echelle spectra of stars in three open clusters obtained with the Hydra multiobject spectrograph on the WIYN 3.5 m telescope. Abundances of Fe, O, Si, Ca, Na, Al, and Ni have been determined via equivalent width analysis and spectrum synthesis. Mean abundances for each cluster are compared to those of previous studies and of other clusters in the literature, with emphasis on exploring the enhancements of Na and Al seen in many open clusters. All three clusters show enhanced values of [Na/Fe] and [Al/Fe], while the abundances of Fe, O, Si, and Ca are consistent with their ages and locations in the Galactic disk.

Key words: Galaxy: abundances — open clusters and associations: individual (NGC 7142, NGC 6939, IC 4756) — stars: abundances

Online material: color figures, machine-readable table

1. INTRODUCTION

The unique characteristics of open clusters as a population make them ideal laboratories in which to study a variety of astrophysical problems. Astronomers have long used open clusters to study details of stellar interior physics and galaxy formation and evolution, and the broad spectrum of physical processes in between. That said, the work to determine the most fundamental characteristics of open clusters is still ongoing (see, e.g., the work of Anthony-Twarog, Twarog, and coworkers, the Bologna Open Cluster Chemical Evolution [BOCCE] project, and the WIYN Open Cluster Study).

Of the ~ 30 or so open clusters that have been subject to detailed abundance study, roughly 65% or more show enhanced abundances (~ 0.2 dex) of light elements such as sodium and aluminum (see, e.g., Friel et al. 2003, 2005; Carraro et al. 2004; Tautvaisiene et al. 2000, 2005). Most of these clusters are Hyades-aged or older. These enhancements, which are seen in the brighter, evolved cluster stars that are most easily targeted for such study, may be the result of dredge-up (Tautvaisiene et al. 2000). Whether this phenomenon is indeed only a question of stellar interior physics is not yet clear. Theory does not predict mixing to occur in metal-rich evolved stars (El Eid & Champagne 1995), and because few studies also obtain spectra of dwarf cluster members, a primordial enrichment of light elements often cannot be ruled out. One cluster study, that of IC 4651, included both dwarfs and giants and did see a ~ 0.2 dex enhancement of light elements in giants relative to dwarfs, but a sample size of one cluster is too small to draw conclusions (Pasquini et al. 2004). To further confuse the issue, LTE abundances of light elements are sometimes viewed with skepticism, and the large enhancements seen in evolved stars may be due to the inappropriate assumption of LTE conditions in stellar atmospheres (Sestito et al. 2007).

To disentangle the above effects, it would be helpful to know just how many open clusters exhibit enhancements of light elements, and if there is any correlation between enhancement and any physical parameter such as age or location in the Galaxy. Therefore, we have undertaken a study of three open clusters in order to see if they also exhibit enhancements. These clusters are NGC 7142, IC 4756, and NGC 6939. Of the three, only IC 4756 has previously been subject to detailed abundance analysis.

2. TARGET CLUSTERS AND OBSERVATIONAL DATA

2.1. Cluster Properties

2.1.1. NGC 7142

NGC 7142 ($l = 105^\circ$, $b = +9^\circ$) is a little-studied, older open cluster (aged ~ 4 Gyr; Salaris et al. 2004). It lies in a region of variable absorption that was explored in detail by Risley (1943). Sharov (1965) performed star counts of the cluster and reported evidence of variable extinction across the cluster. The early photographic and photoelectric studies of NGC 7142 were limited to the brighter stars in the field, and the scatter in the color-magnitude diagrams (CMDs) due to variable extinction and photometric quality made it difficult to derive cluster parameters (see, e.g., Hoag et al. 1961; van den Bergh 1962). In their photometric study of the cluster, van den Bergh & Heeringa (1970) noted NGC 7142's similarity in morphology to M67, and the adoption of M67's evolutionary track allowed for the determination of cluster parameters: $(m - M)_0 = 12.5$, $E(B - V) = 0.41$, and $d = 3.2$ kpc.

Jennens & Helfer (1975) obtained *UBV* photometry of five K giants in the cluster field and determined $E(B - V) = 0.29$ and $[\text{Fe}/\text{H}] = -0.45 \pm 0.20$. Based on Washington photometry of eight stars in the field, Canerna et al. (1986) found $[\text{A}/\text{H}] \sim -0.1$. Typical uncertainties in their sample were ~ 0.1 dex, although the large uncertainty in NGC 7142's reddening might make its metallicity more uncertain (see, e.g., their Fig. 5). Friel et al. (1989) determined radial velocities for 13 stars in the region, and found a mean $V_r = -44 \pm 12$ km s⁻¹ for 12 members, although

¹ Any opinions, findings, conclusions, and recommendations expressed in this material are those of the author and do not necessarily reflect the views of the National Science Foundation.

TABLE 1
 NGC 7142 STARS OBSERVED

ID ^a	ID ^b	V	$B - V$	$V - K$	$J - K$	S/N ^c	V_{rad} (km s ⁻¹)	Membership
95.....	10	13.44	0.64	1.62	0.36	100	-10.7	NM
136.....	8	13.45	0.71	1.79	0.41	130	-15.4	NM
170.....	15	13.71	1.47	3.46	0.79	100	-39.7	M?
171.....	225	12.97	0.85	1.90	0.40	150	-32.9	NM
173.....	4	12.72	1.53	3.56	0.89	90	-48.4	M
196.....	98	13.43	1.59	3.67	0.88	90	-49.3	M
203.....	192	13.79	1.37	3.17	0.72	100	-46.4	M
229.....	222	12.71	1.79	4.19	1.00	100	-49.5	M
231.....	2	11.14	0.88	3.55	0.77	200	+6.9	NM
262.....	1	13.60	0.62	4.71	0.32	250	-33.9	NM
278.....	12	13.58	0.71	1.69	0.34	100	-31.9	NM
333.....	175	13.65	0.72	1.89	0.41	30	-29.6	NM
349.....	1349	13.92	0.78	2.06	0.42	80	-86.9	NM
377.....	7	13.08	1.67	3.84	0.96	100	-49.3	M
387.....	211	13.40	0.76	2.00	0.45	40	-56.0	M?
399.....	210	13.48	1.43	3.40	0.84	150	-21.2	NM
421.....	9	13.43	1.41	3.30	0.80	100	-48.6	M

^a Identification from CT91.

^b Identification used in WEBDA.

^c Average of Na and Al data.

they stressed that their errors were 10–15 km s⁻¹. Friel & Janes (1993) determined metallicities of 13 stars in the region from medium-resolution spectroscopy. They reported a mean $[\text{Fe}/\text{H}] = -0.23 \pm 0.13$ for 11 cluster members. Twarog et al. (1997) transformed the spectroscopic abundances of the 11 cluster members from Friel et al. (1989) to their revised metallicity scale and found a mean $[\text{Fe}/\text{H}] = +0.04$ (SEM 0.02 dex.)

The only published CCD photometric study of this cluster was done by Crinklaw & Talbert (1991, hereafter CT91). Their BV photometry extends to $V \sim 18$, with considerable scatter in the CMD. They estimated differential extinction across the cluster on the order of 0.1 mag, based on the width of the main sequence. Adopting $[\text{Fe}/\text{H}] = -0.1$ (Canterna et al. 1986) and $E(B - V) = 0.41$ (van den Bergh & Heeringa 1970), they derived $(m - M)_0 = 11.4 \pm 0.9$ via main-sequence fitting.

Targets for our study of NGC 7142 were chosen based on CT91's photometry and identifications (see Table 1; obtained from the WEBDA² database). Adopting $E(B - V) = 0.41$ and $(m - M)_0 = 11.9$, NGC 7142 lies 9.1 kpc from the Galactic center and about 300 pc above the plane. The CMD for NGC 7142 is shown in Figure 1, with the targets of this study identified.

2.1.2. NGC 6939

Several studies of cluster NGC 6939 ($l = 95^\circ$, $b = +12^\circ$) are available in the literature. Kustner (1923) presented the first observations of the cluster, and NGC 6939 has been subject to several photographic, photoelectric, and CCD studies since (e.g., Chincarini 1963; Cannon & Lloyd 1969; Mermilliod et al. 1994; Rosvick & Balam 2002, hereafter RB02; Andreuzzi et al. 2004, hereafter A04). Proper-motion studies were carried out by Meurers & Scharf (1957), Cannon & Purcell (1970), and Glushkova & Rastorguev (1991), with the latter two having very similar results.

Radial velocity studies of NGC 6939 have resulted in disparate results. Values range from -42 ± 10 km s⁻¹ (Thogersen et al. 1993, although their uncertainties are large: 10–15 km s⁻¹) to $+5$ km s⁻¹ (Lynga & Lundstrom 1980). The studies of Glushkova

& Rastorguev (1991) and Milone (1994), among others, consistently gave a mean value of about -19 km s⁻¹ for the cluster. Thogersen et al. (1993) determined $[\text{Fe}/\text{H}] = -0.14 \pm 0.13$ from spectroscopic indices, and this value was transformed to -0.19 ± 0.09 in Friel et al. (2002). Twarog et al. (1997) also transformed the Thogersen et al. value onto their scale, which resulted in a slightly higher metallicity: $[\text{Fe}/\text{H}] = +0.03$ (SEM 0.06). Canterna et al. (1986) found a mean $[\text{A}/\text{H}] = -0.1 \pm 0.1$ from Washington photometry of 11 stars.

The two most recent photometric studies have been done by RB02 and A04. RB02 obtained BVI data down to $V = 20$ and derived $(m - M)_V = 12.27 \pm 0.41$ and $E(B - V) = 0.33 \pm 0.07$.

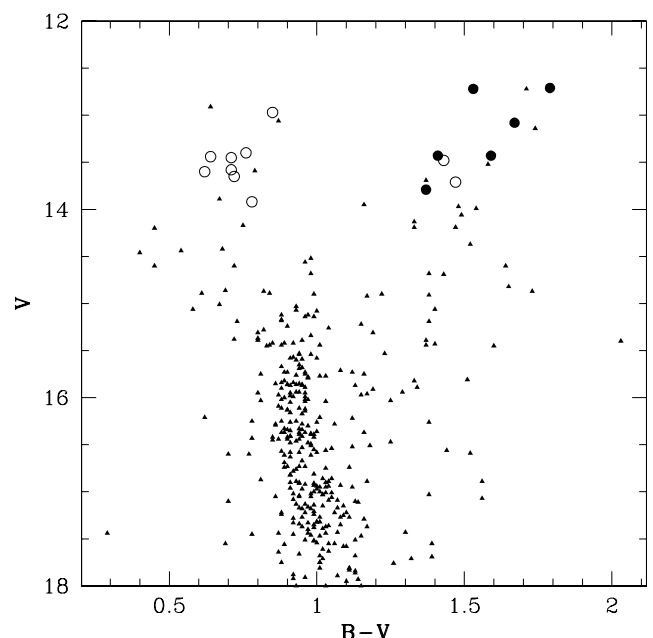


FIG. 1.—CMD of NGC 7142 using the photometry of CT91. Target stars are circles: filled circles are members, and open circles are nonmembers. [See the electronic edition of the Journal for a color version of this figure.]

² See <http://www.univie.ac.at/webda/webda.html>.

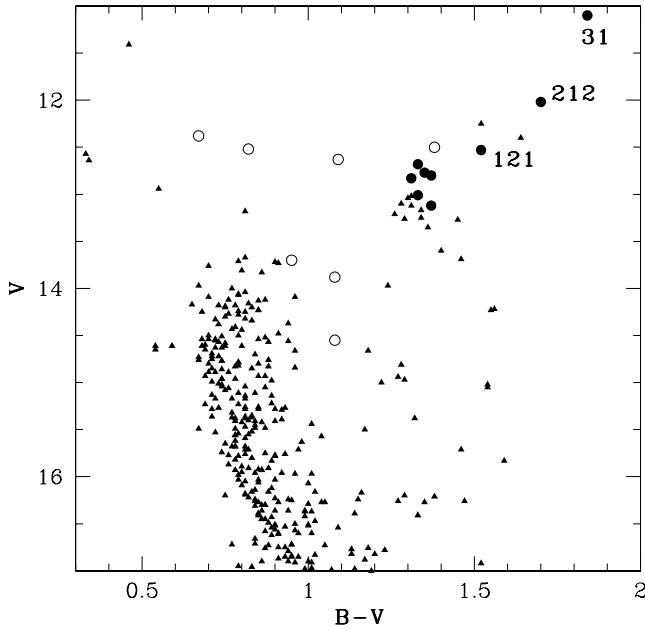


FIG. 2.—CMD of NGC 6939 using A04. Target stars are circles: filled circles are members, and open circles are nonmembers. [See the electronic edition of the *Journal* for a color version of this figure.]

They also reported strong indications of variable extinction across the cluster, not only evidenced by the width and shape of the main sequence and red clump, but seen in comparison of CMDs made using stars in different quadrants of the field. A04, however, found no evidence of differential extinction in their *UBVI* data. By generating synthetic CMDs, they determined the best-fitting parameters for NGC 6939 to be $E(B - V) = 0.34 - 0.38$, $(m - M)_0 = 11.3 - 11.4$, age = 1–1.3 Gyr, and solar metallicity. These values place NGC 6939 about 8.4 kpc from the Galactic center and 400 pc above the plane.

For this study, we adopt the V , $B - V$ data of A04 for the target stars available from the WEBDA database. Likely cluster

members were identified via their photometry, and based on the work of Mermilliod et al. (1994) and Glushkova & Rastorguev (1991). A04's CMD of NGC 6939 is shown in Figure 2, with our target stars identified. General photometric information on the stars observed for this study is given in Table 2.

2.1.3. IC 4756

IC 4756 ($l = 36^\circ$, $b = +5^\circ$) is another cluster subject to variable extinction (Schmidt 1978; Smith 1983). Herzog et al. (1975) presented photographic *UBV* photometry, proper motions, and membership probabilities for over 400 stars in the field. As pointed out by Twarog et al. (1997), scatter in the CMD makes it somewhat difficult to derive a distance to the cluster, but most estimates are around 400 pc (Herzog et al. 1975; Mermilliod & Mayor 1990, hereafter MM90). Salaris et al. (2004) determined a cluster age of ~ 800 Myr. The CMD of the cluster shown in Figure 3 is based on the photometry of Herzog et al. (1975) obtained from the WEBDA database, with targets of this study identified. Radial velocities studies have been done by Pendl & Seggewiss (1975), MM90, and Thogersen et al. (1993), who found mean cluster velocities of -17.2 , -25.8 ± 0.6 , and -28 ± 11 km s $^{-1}$, respectively. For the eight stars in their study, Thogersen et al. (1993) found a mean $[\text{Fe}/\text{H}] = -0.22 \pm 0.12$. Based on both Thogersen et al.'s data and the DDO photometry of Smith (1983), Twarog et al. (1997) found a weighted average $[\text{Fe}/\text{H}] = -0.060 \pm 0.102$ for the cluster. Luck (1994) determined $[\text{Fe}/\text{H}] = -0.03 \pm 0.06$ from four likely members, as well as abundances of several other elements.

Targets for this project were chosen based on the radial velocity and proper motion cluster membership data of MM90 and Herzog et al. (1975). Basic data for stars in IC 4756 are presented in Table 3, with V , $B - V$ data taken from Herzog et al. (1975). In a study of carbon isotope ratios and lithium abundances of open clusters, Gilroy (1989) obtained spectra of seven cluster members, all of which are included in this study, and determined a cluster mean $[\text{Fe}/\text{H}] = +0.04 \pm 0.08$. We also have three stars in common with Luck (1994). For this study, we adopted the cluster parameters presented in Gilroy (1989): $(m - M)_0 = 8.25$,

TABLE 2
NGC 6939 STARS OBSERVED

ID ^a	V	$B - V$	$V - K$	$J - K$	S/N ^b	V_{rad} (km s $^{-1}$)	Membership
31.....	11.10	1.84	4.35	1.11	150	-18.4	M
36.....	12.60	0.73	2.06	0.43	40	-20.9	NM ^c
53.....	12.80	1.30	3.09	0.76	100	-18.8	M
59.....	12.40	0.56	1.60	0.36	110	+0.8	NM
65.....	12.70	1.30	3.10	0.60	130	-17.5	M
80.....	13.90	1.05	2.78	0.62	80	-40.1	NM
83.....	14.50	1.08	2.60	0.59	75	+1.0	NM
109.....	13.70	0.94	1.20	0.49	90	-14.9	NM, binary?
121.....	12.50	1.54	3.70	0.90	110	-19.4	M
135.....	12.60	1.11	2.88	0.66	100	1.2	NM
182.....	12.90	1.37	3.30	0.70	110	-13.7	M?
190.....	12.70	1.36	3.01	0.72	130	-20.1	M
212.....	12.00	1.69	4.00	1.00	120	-18.0	M
230.....	12.90	1.32	3.06	0.74	110	-17.1	M
292.....	13.20	1.36	3.40	0.80	80	-17.9	M
301.....	12.50	1.38	3.44	0.84	120	-30.3	NM

^a Identification used in WEBDA (Kustner 1923).

^b Average value of Na and Al data.

^c Proper motion NM (Mermilliod et al. 1994).

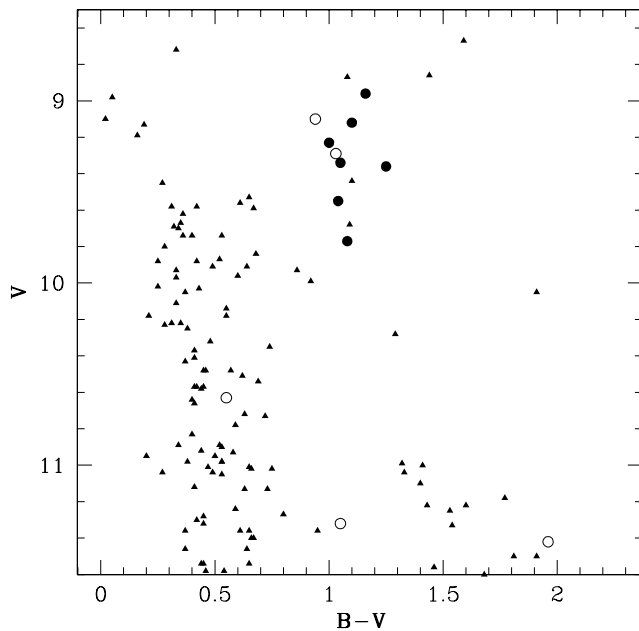


FIG. 3.—CMD of IC 4756 using the photometry of Herzog et al. (1975). Target stars are circles: filled circles are members, and open circles are nonmembers. [See the electronic edition of the *Journal* for a color version of this figure.]

$E(B - V) = 0.21$, age 800 ± 160 Myr, and main-sequence turnoff mass $2.2 \pm 0.4 M_{\odot}$. Gilroy determined these parameters by fitting Vandenberg (1985) isochrones to the Herzog et al. (1975) CMD. These values place IC 4756 8.1 kpc from the Galactic center and 37 pc above the plane.

2.2. Description of Data

Single-order echelle spectra of stars in each cluster were obtained with the Hydra multiobject spectrograph on the WIYN 3.5 m telescope in the fall of 2005. Spectra centered around the Na $\lambda\lambda 6154, 6160$ and Al $\lambda\lambda 6696, 6698$ doublets were obtained on September 11–14, and spectra centered around the [O I] $\lambda 6300$ forbidden feature were obtained on October 14–15. Oxygen data were obtained for NGC 7142 and NGC 6939 only; IC 4756 was no longer observable. The typical spectral resolution of the three regions is $R \sim 15,000$, and individual exposure times range from 30 to 60 minutes.

The data were reduced using normal IRAF³ routines. Individual exposures were trimmed, bias-subtracted, and flat-field corrected, and apertures were extracted. After wavelength calibration, sky subtraction, and continuum placement, individual exposures of each aperture were combined into a single, higher S/N ($70\text{--}150 \text{ pixel}^{-1}$) spectrum for each star. Wavelength coverage of each spectral region is about 300 Å. Sample spectra are shown in Figure 4.

3. ANALYSIS

3.1. Stellar Radial Velocities and Membership

Radial velocities for the program stars were measured using IRAF *fxcor*. After normalization and apodization of the spectrum, the linear wavelength scale is transformed to a log scale; a cross-correlation of the spectrum with a template is performed; and a Gaussian is fit to the upper 50% of the cross-correlation peak. A twilight sky spectrum was used as a template for cross-correlation. The measured radial velocity values were used to verify cluster membership. The final stellar velocities given in Tables 1–3 are averages of the cross-correlation results against both the Na and Al spectra.

Cluster members and average cluster radial velocities were determined by examination of histograms of the radial velocities. The average radial velocity for each cluster from stars taken to be cluster members is $-48.6 \pm 1.1 \text{ km s}^{-1}$ (six stars), $-18.4 \pm 1.0 \text{ km s}^{-1}$ (eight stars), and $-24.9 \pm 1.4 \text{ km s}^{-1}$ (six stars) for NGC 7142, NGC 6939, and IC 4756, respectively. For NGC 7142 our study has four stars in common with that of Friel et al. (1989). The average radial velocity of these four stars, $-46.7 \pm 4.7 \text{ km s}^{-1}$, is consistent with that found by Friel et al. (1989; $-49.5 \pm 14.4 \text{ km s}^{-1}$) from lower resolution spectra. Similarly, our average cluster value for NGC 6939 agrees well with that found by Milone (1994): $-18.98 \pm 0.19 \text{ km s}^{-1}$. Star 36 in NGC 6939 has a radial velocity consistent with the cluster average, but the proper-motion study of Mermilliod et al. (1994) indicates it is not a member. Spectroscopic analysis later confirmed this. The Mermilliod et al. study indicated star 135 as a cluster member, but its radial velocity indicates it is either a non-member or a binary. Star 109 shows evidence of binarity. Finally, although its radial velocity indicates it is likely a nonmember, we

³ IRAF is distributed by the National Optical Astronomy Observatory, which is operated by the Association of Universities for Research in Astronomy, Inc., under cooperative agreement with the National Science Foundation.

TABLE 3
IC 4756 STARS OBSERVED

ID ^a	V	$B - V$	$V - K$	$J - K$	S/N ^b	V_{rad} (km s^{-1})	V_{rad} (MM90)	Membership
44 ^c	9.77	1.08	2.66	0.63	130	-25.0	-26.61	M
48.....	9.10	0.94	2.38	0.55	200	-22.4	-22.53	NM
49.....	9.36	1.25	2.82	0.67	100	-24.4	-25.91	M
69.....	9.12	1.10	2.70	0.61	140	-27.7	-25.47	M, binary
88.....	10.63	0.55	1.15	0.22	100	+16.0	...	NM
101.....	9.34	1.05	2.56	0.61	100	-24.7	-26.41	M
109.....	8.96	1.16	2.71	0.66	130	-23.9	-25.92	M
125.....	9.23	1.00	2.55	0.64	140	-24.0	-25.46	M
139.....	9.55	1.04	2.58	0.59	60	-26.5	-27.01	M (S. B.)
254.....	11.32	1.05	2.68	0.72	120	-42.4	...	NM
1356.....	11.42	1.96	4.77	1.18	50	-18.1	...	NM

^a Identification used in WEBDA, Kopff (1943).

^b Average value of Na and Al data.

^c Photometry from Alcaino (1965).

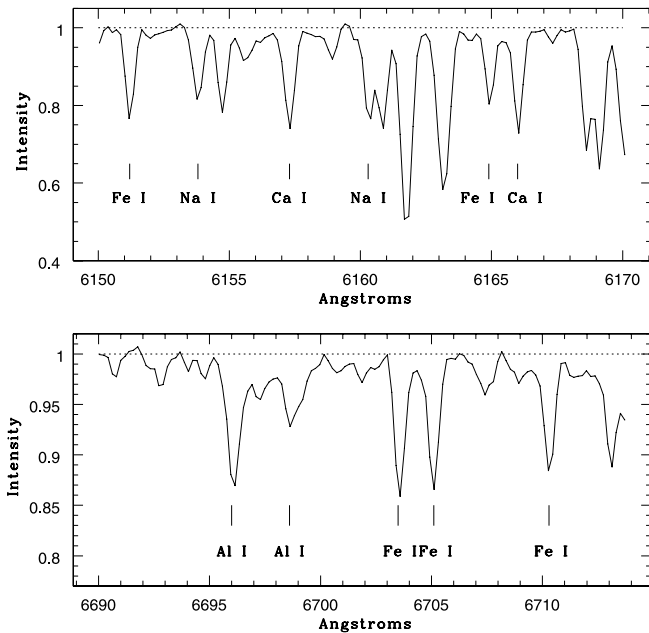


FIG. 4.—*Top*: Region around the Na $\lambda\lambda$ 6154, 6160 doublet in the spectrum of star NGC 6939-230. *Bottom*: Region around the Al $\lambda\lambda$ 6696, 6698 doublet in the spectrum of star IC 4756-125. The continuum is indicated by the dotted line, and key lines are identified.

carried out an abundance analysis of star 182. It is excluded from all calculations of average cluster properties.

For IC 4756, Table 3 also shows radial velocities for target stars determined by MM90 for comparison. The agreement between the two studies is quite good. All observed stars save 254 were declared proper-motion members by Herzog et al. (1975). Star 139 is a spectroscopic binary, and was not included in further analysis. MM90 determined star 48 likely to be a nonmember; our spectroscopic analysis supports this.

To estimate systematic errors, we cross-correlated twilight sky spectra from different nights and found relative velocities smaller than 1.1 km s^{-1} . Cross-correlation of individual apertures in a twilight sky spectrum showed velocity variations less than 0.5 km s^{-1} . Uncertainties may arise from using a dwarf star template against giant star spectra. We combined the spectra of five NGC 6939 stars into a single high-S/N spectrum and cross-correlated it against NGC 7142 and IC 4756 stars. Results differed from those using the solar template by less than 1.5 km s^{-1} . We conclude that the internal errors on the radial velocity measurements are $1\text{--}2 \text{ km s}^{-1}$. We have no way of determining any zero-point offsets in our analysis. The good agreement between our results and those of other studies implies that any offset is small.

3.2. Line List and Equivalent Widths

We have followed the same methods for measurement of equivalent widths and abundance analysis as for Cr 261 and Be 17. Only a brief summary of the method is necessary here; the reader is referred to our previous papers (Friel et al. 2003, 2005) for further details.

All gf -values in our line list are derived relative to Arcturus, adopting the abundances and atmospheric parameters determined in Peterson & Green (1998; see Table 2 in Friel et al. 2003). We note here that $\log gf$ of Na I λ 6160.75 has been modified in this work based on a revised measurement of its equivalent width in the Arcturus spectrum (Hinkle et al. 2000; $96.7 \text{ m}\text{\AA}$ instead of $88.8 \text{ m}\text{\AA}$; the new line strength was confirmed by spectrum synthesis.) The full line list and measured equivalent widths in the stars are given in Table 4. We used the LTE abundance program MOOG (Snedden 1973; 2002 version) to determine abundances. Model atmospheres were interpolated from the grid of Bell et al. (1976) for the preliminary T_{eff} and $\log g$ values estimated from photometry for each cluster.

Equivalent widths (EWs) for all stars were measured from the extracted spectra using the interactive routines in IRAF and fitting Gaussian profiles to each line. Due to the relatively high amount of line blending in these spectra, extreme care was taken in deblending features. Table 5 of Fulbright et al. (2006) was used to aid continuum placement. Only lines weaker than $150 \text{ m}\text{\AA}$ were used for the abundance analysis. However, we provide measurements for several lines that are only slightly above this limit or are from elements, like Na, that have very few lines.

3.3. Atmospheric Parameters

Preliminary values for T_{eff} and $\log g$ were calculated based on available photometry for each cluster: BV for NGC 7142 (CT91), $UBVI$ for NGC 6939 (A04), and UBV for IC 4756 (Herzog et al. 1975). In addition, all stars in each cluster were observed by the Two Micron All Sky Survey (2MASS; Cutri et al. 2003) (see Tables 1–3). The temperature calibrations of Di Benedetto (1998) and Alonso et al. (1999) were used along with the color excesses adopted for each cluster, and the averaged T_{eff} taken as a preliminary value in the spectroscopic analysis.

Initial values of $\log g$ were determined from each star's position in the CMD, assuming the distance modulus chosen for each cluster in §§ 2.1.1–2.1.3, a turnoff mass calculated using the adopted age of the cluster, and bolometric corrections from Alonso et al. (1999). An initial microturbulent velocity of 1.5 km s^{-1} was assumed for every star.

From these initial calculations, the effective temperature, $\log g$ value, and microturbulent velocity were altered by small amounts in an iterative fashion as necessary to remove trends in excitation

TABLE 4
NGC 7142 EQUIVALENT WIDTHS

Element	λ (\AA)	EP	$\log gf$	EW 173 ($\text{m}\text{\AA}$)	EW 196 ($\text{m}\text{\AA}$)	EW 203 ($\text{m}\text{\AA}$)	EW 229 ($\text{m}\text{\AA}$)	EW 377 ($\text{m}\text{\AA}$)	EW 421 ($\text{m}\text{\AA}$)
Na I.....	6154.23	2.10	-1.80	117.0	118.4	86.8	140.0	123.5	114.2
Na I.....	6160.75	2.10	-1.44	139.3	137.5	108.5	162.2	142.5	134.2
Al I.....	6696.03	3.14	-1.44	61.6	111.3	54.1	107.7	93.4	88.4
Al I.....	6698.67	3.13	-1.94	80.9	79.7	35.2	95.9	84.4	50.3
Si I.....	6142.49	5.62	-1.86	66.8	41.9	52.7	40.0	30.4	66.4

NOTES.—Table 4 is published in its entirety in the electronic edition of the *Astronomical Journal*. A portion is shown here for guidance regarding its form and content.

TABLE 5
NGC 7142: ADOPTED ATMOSPHERIC PARAMETERS

Star	T_{eff} (K)	$\log g$ (dex)	v_t (km s ⁻¹)
173.....	4650	2.1	1.5
196.....	4600	2.0	1.5
203.....	5250	3.0	1.8
229*	4500	2.3	1.9
377.....	4550	2.3	1.5
421.....	5000	2.8	2.0

NOTE.—The asterisk indicates more uncertain parameters; see text.

potential, ionization equilibrium, or equivalent width, respectively, for the Fe lines. Final, spectroscopically determined atmospheric parameters for stars in NGC 7142, NGC 6939, and IC 4756 are given in Tables 5, 6, and 7, respectively.

In the case of IC 4756, for which we have no oxygen spectra, the $\log g$ determination is based on three Fe II lines and is therefore less robust than for stars in the other two clusters. For some relatively cool, strong-lined stars, it was very difficult to disentangle the effects of T_{eff} and v_t in trends with equivalent width, as the weaker lines have the highest excitation potential (EP) values. As a result, the derived atmospheric parameters for these stars are more uncertain. These stars are marked with an asterisk in Tables 5–12.

The differences between photometric and spectroscopic parameters varied greatly across the whole sample, and within clusters as well. In general, spectroscopic temperatures were usually higher, on the order of 100–200 K. The differences were not a function of temperature. For most stars, the $(J - K)$ -derived temperature was most similar to the spectroscopic temperatures (within ~ 100 K); the $(J - H)$, $(V - K)$, and $(B - V)$ temperatures were usually more discrepant. It is not surprising that the $(B - V)$ temperatures were much different considering the effects of suspected variable extinction or the quality of the photometry used for two of these clusters. The NGC 6939 stars were the exception to this; for the most part their $(B - V)$ temperatures agreed well with the spectroscopic and $(J - K)$ temperatures. Comparing gravities, spectroscopic gravities were on average much lower than photometric gravities, by 0.5–0.9 dex in some cases.

Five of the six IC 4756 stars were studied by Gilroy (1989) using similar analysis techniques to ours. For comparison, we

TABLE 6
NGC 6939: ADOPTED ATMOSPHERIC PARAMETERS

Star	T_{eff} (K)	$\log g$ (dex)	v_t (km s ⁻¹)
31.....	4150	1.6	1.8
53.....	4920	2.4	1.7
65.....	5100	3.0	1.8
121.....	4500	1.5	1.6
182.....	4900	2.5	1.5
190.....	5050	2.7	2.0
212*	4400	2.0	1.5
230.....	5100	2.9	1.9
292*	5000	2.6	1.6

NOTE.—The asterisks indicate more uncertain parameters; see text.

TABLE 7
IC 4756: ADOPTED ATMOSPHERIC PARAMETERS

STAR	THIS STUDY			GILROY (1989)		
	T_{eff} (K)	$\log g$ (dex)	v_t (km s ⁻¹)	T_{eff} (K)	$\log g$ (dex)	v_t (km s ⁻¹)
44.....	4970	2.2	1.4
49.....	5050	2.5	1.6	5000	2.9	1.8
69.....	5000	2.2	1.5	5200	3.2	2.0
101.....	5100	2.5	1.6	5000	2.9	1.8
109.....	4950	2.0	1.5	5000	2.9	1.8
125.....	5100	2.2	1.6	5000	2.9	1.8

present Gilroy's atmospheric parameters alongside our own in Table 7. On average, our T_{eff} values are the same as Gilroy's, but our $\log g$ values are 0.4–1.0 dex smaller. The cause of the difference in gravities is how they were determined: while ours were determined spectroscopically, Gilroy's $\log g$ values were calculated using the cluster turnoff mass, T_{eff} values, and bolometric magnitudes. Since our spectroscopic gravities are 0.4–0.8 dex lower than our photometric ones, it is not surprising they are lower than Gilroy's values by the same magnitude.

What could cause the spectroscopic $\log g$ values to be so much lower than the photometric ones? A possible culprit could be the small number of Fe II lines used to determine gravity and the quality of their EW measurements. Examination of the Fe II lines in the spectra of these stars confirms that, if there is any blending present, it is slight. (Looking at the Hinkle et al. [2000] Arcturus atlas, there are small features near some of the lines.) We were careful to account for blends in the EW measurement process, including blends with small, unidentified features. Nevertheless, could blends be affecting the EW measurements?

We determined abundances for the five stars in common to our studies using Gilroy's atmospheric parameters and our EWs. On average, the Fe I abundances were ~ 0.1 dex less than for our parameters, and for three of the five stars there was a significant trend of abundance with EP. The Fe II abundances were of order ~ 0.2 dex larger than for our parameters. Let us suppose that Gilroy's (and the photometric) $\log g$ values are correct; the discrepancy between Fe I and Fe II could be caused by the Fe II EWs being too strong. In order for the Fe I and Fe II abundances to agree, the EWs of the Fe II lines would have to be reduced by ~ 10 – 25 mÅ, larger than our estimated measurement uncertainty (§ 3.5). It seems unlikely that blends with small features, which we have already accounted for when measuring, could increase the EWs by ~ 20 mÅ. So, while blends and other systematics may affect our line measurements, we contend that the observed Fe II line strengths are inconsistent with the higher surface gravities used by Gilroy.

Ultimately, an error of 0.9 dex in $\log g$ does not significantly affect our results for the light elements. A change in $\log g$ of 0.5 dex resulted in a change of at most 0.04 dex in the abundance of sodium and aluminum, which is well within our uncertainties. Fe I abundances were more affected: of order ~ 0.11 dex.

Average abundances of Fe, Na, and Al for each star are given in Table 8, along with the standard deviation of the mean and the number of lines for each species. Average cluster abundances are shown in Table 9, again with dispersions about the mean. The Fe abundances reported are calculated using only Fe I lines. Abundances of silicon, calcium, and nickel, for which three to four lines of each were measured, are given in Tables 10 and 11.

TABLE 8
Fe, Na, Al, AND O ABUNDANCES: EW ANALYSIS

STAR	Fe I			Fe II			Na I		Al I		[O I]
	[X/H]	σ	<i>N</i>	[X/H]	σ	<i>N</i>	6154 Å	6160 Å	6696 Å	6698 Å	6300 Å
7142-173	0.09	0.22	22	0.07	0.14	6	0.71	0.65	-0.05	0.14	0.10
7142-196	-0.02	0.20	17	-0.01	0.21	6	0.69	0.60	0.38	0.38	-0.10
7142-203	0.13	0.19	20	-0.01	0.22	7	0.58	0.50	-0.13	0.05	0.15
7142-229*	0.07	0.27	16	0.09	0.14	7	0.71	0.61	0.10	0.43	0.20
7142-377	0.08	0.20	14	0.08	0.11	7	0.68	0.56	0.06	0.41	0.15
7142-421	0.16	0.21	20	0.04	0.13	7	0.75	0.62	0.18	0.15	0.10
6939-31	-0.01	0.24	16	0.31	0.20	5	0.27	0.40	0.19	0.13	-0.10
6939-53	-0.11	0.17	22	0.02	0.10	7	0.34	0.16	0.08	-0.01	-0.25
6939-65	0.03	0.20	22	0.04	0.06	8	0.32	0.30	0.03	0.19	0.0
6939-121	-0.19	0.23	21	-0.14	0.18	5	0.51	0.39	0.39	0.12	...
6939-182	0.21	0.25	22	0.15	0.27	8	0.66	0.64	0.57	0.82	-0.4
6939-190	0.04	0.24	21	-0.02	0.11	7	0.58	0.56	0.04	0.01	-0.2
6939-212*	0.07	0.24	15	0.15	0.10	6	0.48	0.44	0.30	0.17	-0.10
6939-230	0.03	0.35	20	-0.05	0.12	7	0.51	0.39	0.05	0.19	0.0
6939-292*	0.14	0.14	18	-0.11	0.26	8	0.40	0.41	0.21	0.10	-0.1
4756-44	-0.23	0.20	24	-0.26	0.12	4	0.37	0.36	0.25	0.20	...
4756-49	-0.12	0.19	21	-0.13	0.15	3	0.40	0.40	0.02	0.04	...
4756-69	-0.15	0.17	23	-0.08	0.16	3	0.45	0.48	0.27	0.16	...
4756-101	-0.17	0.15	22	-0.19	0.01	3	0.41	0.36	0.12	0.06	...
4756-109	-0.12	0.22	18	-0.11	0.09	3	0.54	0.61	0.09	0.23	...
4756-125	-0.12	0.16	23	-0.16	0.15	3	0.37	0.35	0.08	0.14	...

NOTE.—The asterisks indicate more uncertain parameters; see text.

3.4. Spectrum Synthesis

3.4.1. Na and Al

At Hydra's resolution, the Na and Al doublets are both subject to blending in the spectra of these relatively metal-rich stars. Thus, equivalent widths of these blended features can be difficult to determine with confidence, and the resulting abundance determinations can have large uncertainties. While it is reassuring to see that the star-to-star dispersions in the Na and Al abundances are largely near 0.10 dex (Table 9), it is desirable to check the derived abundances using spectrum synthesis.

Spectrum synthesis was performed using MOOG. Synthesis line lists of the regions around the Na and Al doublets were developed from a handful of sources. Atomic parameters for lines that were not in our original line list were obtained from the Vienna Atomic Line Database (VALD; Kupka et al. 2000). CN features near the Al doublet were identified in the Hinkle et al. (2000) Arcturus atlas, and their $\log gf$ values and EPs were kindly provided by B. Plez (2006, private communication; for a description of how the list was assembled, see Hill et al. 2002). The validity of the line lists was checked by comparison of synthetic Arcturus spectra to the Hinkle et al. (2000) spectrum. An example synthesis of an Na line is shown in Figure 5.

Since we have no information about the C and N abundances of these stars, we adopt $[C/H] = -0.2$ and $[N/H] = +0.2$ for typical red giants, as found by Tautvaisiene et al. (2000) in their

study of evolved stars in M67. A set of three synthetic spectra were created at a time, with the abundances of Na and Al varied in steps of 0.10–0.15 dex. In certain cases where the Al doublet was extremely blended, the synthetic Al spectra were varied in steps of up to 0.25 dex. The syntheses were plotted over the actual spectra, and the best-fitting synthesis determined by eye. Plots of the difference between the observed and synthetic spectra were also examined to help identify the best fit. Each line in the Na and Al doublet was synthesized individually, and the resulting abundances were averaged together. The Na and Al abundances determined via synthesis averaged over all stars in each cluster are also shown in Table 9. Note that the Na abundances are not corrected for non-LTE effects (see § 4.2).

Because the Na $\lambda 6154$ line is unblended, we were able to directly compare the abundances for this line derived from the EW and synthesis methods. The following analysis was performed for each star in NGC 7142 and about half the stars in the other two clusters. We measured the equivalent width of the $\lambda 6154$ line in each of the three synthetic spectra using interactive routines in IRAF and compared them to the observed EW measured from the spectrum. We found that the EW measured in the best-fit synthetic spectrum was larger than the observed EW by ~ 7 – 9 mÅ for about 40% of the stars checked. In other words, the synthetic spectrum with an abundance 0.1 dex below that of the best-fit synthetic spectrum had an EW more consistent with the observed EW, for these stars.

TABLE 9
AVERAGE CLUSTER Fe, Na, Al, AND O ABUNDANCES

Cluster	[Fe/H]	[Na/Fe]: EW	[Na/Fe]: Synth.	[Al/Fe]: EW	[Al/Fe]: Synth.	[O/Fe]
NGC 7142	+0.08 ± 0.06	+0.56 ± 0.05	+0.79 ± 0.08	+0.09 ± 0.15	+0.20 ± 0.07	+0.02 ± 0.10
NGC 6939 ^a	+0.00 ± 0.10	+0.40 ± 0.11	+0.43 ± 0.16	+0.14 ± 0.11	+0.17 ± 0.10	-0.11 ± 0.09
IC 4756	-0.15 ± 0.04	+0.57 ± 0.06	+0.63 ± 0.07	+0.29 ± 0.08	+0.18 ± 0.04	...

^a Excluding star 182.

TABLE 10
Si, Ca, AND Ni ABUNDANCES: EW ANALYSIS

STAR	Si I			Ca I			Ni I		
	[X/H]	σ	N	[X/H]	σ	N	[X/H]	σ	N
7142-173	0.55	0.28	3	0.19	0.28	3	0.02	0.29	4
7142-196	0.68	0.42	3	0.16	0.13	3	0.27	0.08	4
7142-203	0.35	0.15	3	0.22	0.13	3	0.24	0.12	4
7142-229*	0.49	0.42	3	0.17	0.20	4
7142-377	0.41	0.43	3	0.21	0.17	2	0.15	0.11	4
7142-421	0.47	0.21	3	0.11	0.06	3	0.13	0.12	4
6939-31	0.53	0.25	2	0.15	0.19	4
6939-53	0.25	0.15	3	0.06	0.18	3	0.04	0.16	4
6939-65	0.34	0.12	3	0.13	0.23	3	0.08	0.11	4
6939-121	0.25	0.19	3	-0.02	0.18	3	-0.19	0.06	4
6939-182	0.47	0.23	3	0.14	0.17	4	0.18	0.13	4
6939-190	0.39	0.24	3	0.08	0.10	3	0.09	0.15	4
6939-212*	0.56	0.43	3	0.09	0.14	4	0.14	0.10	4
6939-230	0.26	0.17	3	0.08	0.18	3	0.04	0.19	4
6939-292*	0.40	0.08	3	0.40	0.04	3	0.43	0.28	4
4756-44	0.10	0.19	3	-0.02	0.12	3	-0.13	0.07	4
4756-49	0.26	0.12	3	0.00	0.02	2	-0.05	0.12	4
4756-69	0.26	0.20	3	-0.17	0.19	3	0.01	0.15	4
4756-101	0.18	0.09	3	-0.15	0.15	3	-0.07	0.11	4
4756-109	0.16	0.17	3	-0.01	0.02	3	-0.12	0.08	4
4756-125	0.16	0.18	3	-0.16	0.15	3	-0.06	0.07	4

NOTE.—The asterisks indicate more uncertain parameters; see text.

The Na λ 6160 line is blended with the Ca I λ 6161.3 line in these spectra, making its EW more uncertain. Nonetheless, we repeated the above analysis for the λ 6160 line. Here too, we found that the EW in the best-fit synthetic spectrum was larger than the observed EW by ~ 7 – 9 mÅ for about 40% of the stars checked; the synthetic spectrum with an abundance 0.1 dex lower resulted in comparable synthetic and observed EWs. For the 12 stars checked, the average abundance difference between the by-eye best-fit synthetic spectrum and the by-EW best-fit synthetic spectrum was 0.03 ± 0.06 (standard deviation).

The Al doublet suffers from a higher degree of blending than the Na lines, and so a similar comparison of synthetic EWs to observed EWs was not possible. Instead, we once again made use of the Hinkle et al. (2000) Arcturus spectrum. We first convolved the high-resolution Arcturus spectrum with a Gaussian to match the resolution of our data, and then generated three synthetic spectra to match it. The aluminum abundances were varied by ± 0.1 dex around $[Al/H] = +0.37$ (Peterson et al. 1993), and we visually confirmed that the $[Al/H] = +0.37$ synthesis best matched the observed spectrum. The EWs were then measured from the Atlas spectrum and from the synthetic spectra using interactive routines in IRAF’s *splot* package, namely, the “deblend” function, and great care was taken to deblend the Al lines from the contaminating Fe and CN lines in a consistent fashion. Comparing the observed and synthesis values, the EWs measured from the $[Al/H] = +0.37$ synthesis were consistently 4–5 mÅ weaker

than the observed EWs, and the EWs measured from the $[Al/H] = +0.47$ synthesis were consistently 2–4 mÅ stronger than the observed EWs. This, along with the discussion about sodium above, implies that there may be a small (≤ 0.1 dex) discrepancy between the synthesis abundance determined by eye and the abundance determined by comparing observed and synthetic EWs for individual lines, at least for some stars. It is worth remembering that the synthesis line lists were verified by comparison of synthetic spectra to the *unsmoothed* Hinkle et al. (2000) spectrum and ensuring that the measured EWs of each were consistent.

Figure 6 shows the abundances determined via spectrum synthesis versus those determined via EW analysis for both sodium and aluminum. The solid line shows a one-to-one correlation. Because of the small number of stars observed in each cluster, only general trends shown by the whole sample can be explored. For aluminum, there is large scatter, but overall the trend follows a one-to-one correlation. Sodium abundances also follow a one-to-one correlation except for the highest abundances. For these, the synthesis abundances are systematically higher. This effect may not be real, however; the average difference is less than 0.1 dex, below our uncertainties, and we are likely still dealing with small number statistics.

To better quantify this difference between synthetic and EW abundances, we plotted $\Delta[Na/H] = [Na/H]_{\text{synth}} - [Na/H]_{\text{EW}}$ versus T_{eff} and EW. There was no trend of abundance difference with either temperature or line strength, except for the coolest

TABLE 11
AVERAGE CLUSTER Si, Ca, AND Ni ABUNDANCES

Cluster	[Si/H]	[Si/Fe]	[Ca/H]	[Ca/Fe]	[Ni/H]	[Ni/Fe]
NGC 7142	$+0.49 \pm 0.11$	$+0.41 \pm 0.11$	$+0.18 \pm 0.04$	$+0.11 \pm 0.04$	$+0.16 \pm 0.09$	$+0.08 \pm 0.09$
NGC 6939 ^a	$+0.37 \pm 0.12$	$+0.37 \pm 0.12$	$+0.12 \pm 0.13$	$+0.12 \pm 0.13$	$+0.10 \pm 0.17$	$+0.10 \pm 0.17$
IC 4756	$+0.19 \pm 0.06$	$+0.34 \pm 0.06$	-0.08 ± 0.08	$+0.07 \pm 0.08$	-0.07 ± 0.05	$+0.08 \pm 0.05$

^a Excluding star 182.

TABLE 12
UNCERTAINTIES DUE TO ATMOSPHERIC PARAMETERS

Star	[X/H]	$T_{\text{eff}} + 100 \text{ K}$	$\log g + 0.2 \text{ dex}$	$v_t + 0.3 \text{ km s}^{-1}$	Total
6939-65	Fe I	+0.08	+0.01	-0.09	+0.12
	Fe II	-0.07	+0.10	-0.08	+0.14
	Na I	+0.06	-0.02	-0.05	+0.08
	Al I	+0.05	-0.01	-0.04	+0.06
	Si I	-0.02	+0.02	-0.04	+0.05
	Ca I	-0.08	-0.02	-0.12	+0.14
6939-212*	Ni I	-0.04	+0.02	-0.07	+0.08
	Fe I	+0.01	+0.05	-0.14	+0.15
	Fe II	-0.16	+0.12	-0.10	+0.22
	Na I	+0.10	-0.02	-0.10	+0.14
	Al I	+0.09	+0.0	-0.08	+0.12
	Si I	-0.07	+0.04	-0.06	+0.10
Ca I	+0.13	-0.02	-0.18	+0.22	
Ni I	-0.01	+0.05	-0.13	+0.14	

NOTE.—The asterisk indicates more uncertain parameters; see text.

stars in NGC 7142, the most metal-rich of the three clusters. In this latter case, blends are stronger, and it is possible that some blended features are not included in our synthesis line list.

3.4.2. Oxygen

Oxygen abundances for stars in NGC 7142 and NGC 6939 were determined via synthesis of the [O I] $\lambda 6300.3$ line. The [O I] $\lambda 6363.8$ line was too weak and blended for an abundance to be determined with any degree of certainty. The target star spectra were divided by a single high-S/N “hot star” spectrum to correct for telluric contamination. The “hot star” spectrum was generated by combining the spectra of eight individual A and B stars observed in NGC 1502, a young open cluster observed during the same two nights.

The method of analysis was identical to that described in the previous section. The line list used to synthesize the region was

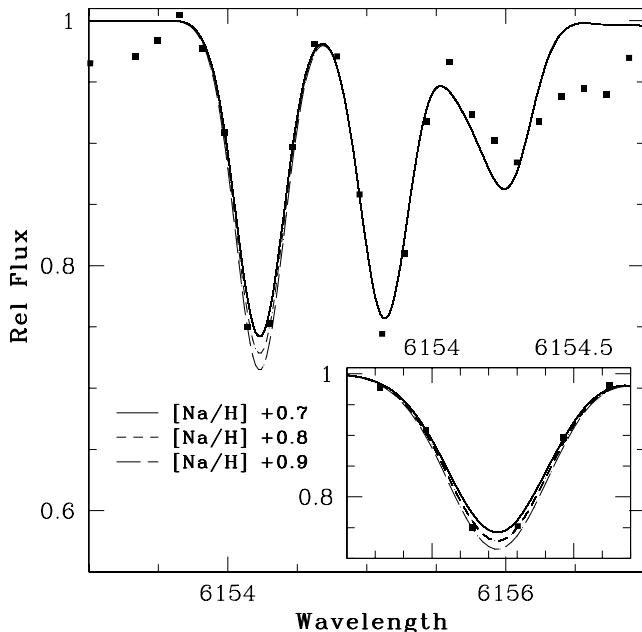


FIG. 5.—Synthesis of the 6154 Å Na line for star NGC 7142-173. Squares represent the actual spectrum; solid, dotted, and dashed lines represent $[\text{Na}/\text{H}] = +0.7, +0.8,$ and $+0.9$ syntheses, respectively. [See the electronic edition of the Journal for a color version of this figure.]

the same used for Cr 261 and Be 17 stars, provided by C. Sneden (2003, private communication). Because of the formation of CO, oxygen abundances are dependent on carbon abundances assumed in the analysis. As before, we assume $[\text{C}/\text{H}] = -0.2$ dex for these evolved stars, as found by Tautvaisiene et al. (2000). With the carbon abundance thus fixed, oxygen abundances were varied in steps of 0.1–0.2 dex, and the resulting syntheses plotted over the telluric-corrected spectra. The best-fit synthesis was then determined by eye. Oxygen abundances are shown in Tables 8 and 9. As found in our work on Cr 261 and Be 17, uncertainties in the carbon abundance have a negligible affect on oxygen abundances.

3.5. Error Budget

Table 12 shows the dependence of abundances on uncertainties in atmospheric parameters for NGC 6939 stars 65 and 212 for the EW analysis. We estimate our effective temperatures to be accurate to 100 K, $\log g$ to 0.2 dex, and microturbulence to 0.3 km s^{-1} ,

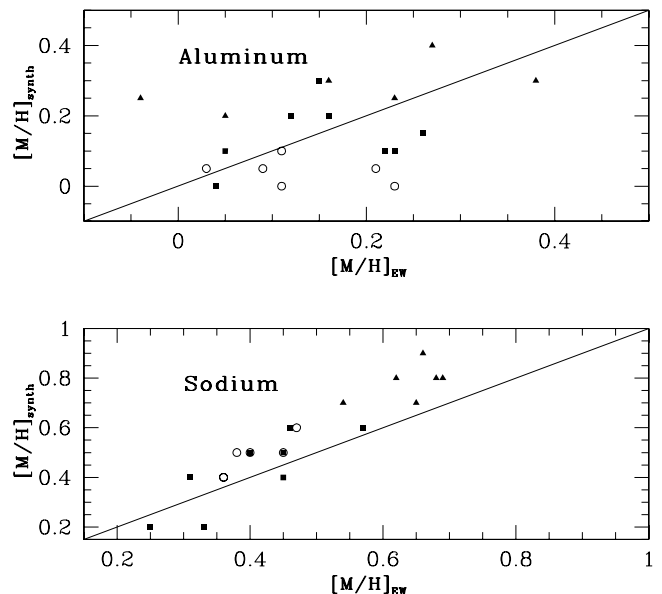


FIG. 6.—Na and Al abundances determined via synthesis vs. those determined via EW analysis. Triangles represent NGC 7142 stars, squares the NGC 6939 stars, and circles the IC 4756 stars. [See the electronic edition of the Journal for a color version of this figure.]

TABLE 13
UNCERTAINTIES IN SYNTHESIS ANALYSIS

Parameter	Sodium (dex)	Aluminum (dex)	Oxygen (dex)
Fitting error.....	0.06	0.09	0.10
Smoothing error.....	0.08	0.04	0.05
$T_{\text{eff}} + 100$ K.....	0.09	0.08	0.03
$\log g + 0.2$ dex.....	0.01	0.01	0.06
$v_t + 0.3$ km s ⁻¹	0.09	0.06	0.04
Total	0.16	0.14	0.14

although the uncertainties may be larger for a few stars (indicated by asterisks in Tables 5–12). A measure of the uncertainty in abundances due to error in equivalent width measurements may be estimated from the standard error of the mean abundance calculated from individual spectral lines: ~ 0.05 dex for Fe I and II, and up to ~ 0.15 dex for elements such as Si and Ca (Tables 8 and 10). Individual EW measurements have an average uncertainty of 3–5 mÅ, based on multiple measurements of spectral lines.

The abundance uncertainties that arise in the synthesis analysis are shown in Table 13. In addition to uncertainties in atmospheric parameters, errors relating to matching the synthetic spectra to the observed spectra and determining the best-fit synthetic spectrum also contribute to abundance uncertainties. To quantify the contribution of each of these uncertainties, we treated each parameter independently and determined uncertainties for five randomly selected stars in our sample. Table 13 shows the average changes in abundances due to each uncertainty.

First of all, the uncertainty in determining the best-fit synthetic spectrum was determined as follows. Recall that three synthetic spectra were generated at one time, with the element abundance varied in steps of 0.1–0.25 dex. After the best-fit synthetic spectrum was determined by eye, the abundance difference between the three synthetic spectra was decreased until we could no longer determine which was the best fit to the observed spectrum. This abundance difference was then adopted as the abundance uncertainty due to the fitting method. For Na and Al, the fitting uncertainties for each line were propagated through the average to determine the average fitting uncertainty.

The synthetic spectra were convolved with Gaussians to match the resolution of the data. If the synthetic spectra do not match the observed spectra’s resolution, the determined abundance may be incorrect. For each star, the size of the Gaussian used for smoothing was determined as follows. In MOOG, a synthetic spectrum ~ 15 – 25 Å in size around each Na, Al, and O feature was plotted over the actual spectrum, and the rms of the difference between the synthetic and observed spectra was calculated. The FWHM of the synthetic spectrum was varied in increments of 0.05, and the FWHM that resulted in the smallest rms value was used for smoothing. We adopt 0.05 as the uncertainty in the FWHM of the smoothing. The resulting abundance uncertainties are shown in Table 13.

The total error shown in Table 13 is calculated by adding the individual errors in quadrature. It is ~ 0.15 dex per element per star.

4. RESULTS AND DISCUSSION

4.1. Comparison to Other Studies

While various studies have determined [Fe/H] for all three of these clusters, we could only find abundances of non-Fe elements reported in the literature for IC 4756. As previously mentioned,

these are the studies of Gilroy (1989) and Luck (1994). Both studies carried out detailed LTE abundance analyses and therefore can be compared to our analysis without any NLTE corrections.

We have determined near-solar Fe abundances for all three clusters (see Table 9). Our slightly supersolar [Fe/H] = 0.08 ± 0.06 for NGC 7142 agrees quite well with that reported by Twarog et al. (1997; [Fe/H] = $+0.04$, SEM 0.02) based on the work of Friel et al. (1989). NGC 6939 has [Fe/H] = 0.00 ± 0.10 , which is consistent with values found by other studies discussed in § 2.1.2. IC 4756 is the most Fe-poor cluster in our sample, with [Fe/H] = -0.15 ± 0.04 . Our value agrees well with the Thogersen et al. (1993) value transformed to the Twarog et al. (1997) system ([Fe/H] ~ -0.11), but is smaller than the approximately solar values found by Gilroy (1989) and Luck (1994).

We found [Na/Fe] $\sim +0.6$ for IC 4756, based on EW and spectrum synthesis analyses. Based on four stars, Luck (1994) determined $\langle [\text{Na}/\text{Fe}] \rangle = +0.11 \pm 0.05$, 0.5 dex smaller than our value. Part of this discrepancy is caused by the difference in our [Fe/H] values. It is more useful to compare [Na/H] values: we determined [Na/H] = $+0.42 \pm 0.06$ (EW analysis), while Luck (1994) found [Na/H] = $+0.08 \pm 0.05$. Looking more specifically at the one star we have in common, star 49, we found [Na/H] = $+0.40 \pm 0.03$, while Luck (1994) reported [Na/H] = $+0.13 \pm 0.19$. The difference in [Na/H] abundance can largely be explained by the different gf -values used: ours were derived relative to Arcturus, while those used by Luck (1994) are derived relative to the Sun, with the result that ours are 0.2 and 0.3 dex larger for the $\lambda 6154$ and $\lambda 6160$ lines, respectively. If we instead used the $\log gf$ values for these lines given in Randich et al. (2006) or VALD, our sodium abundance for star 49 decreased to [Na/H] = $+0.20$, which is consistent with that found by Luck (1994) within the errors.

For aluminum, we determined a mean [Al/Fe] $\sim +0.2$ for IC 4756 for both EW and spectrum synthesis analysis. Luck (1994) found $\langle [\text{Al}/\text{Fe}] \rangle = +0.02 \pm 0.14$. Comparing [Al/H] values, we found [Al/H] = $+0.14 \pm 0.08$ (EW analysis) or [Al/H] = $+0.03 \pm 0.04$ (synthesis), while Luck reported [Al/H] = $+0.05 \pm 0.14$. Within uncertainties, our results are consistent with one another.

Finally, our Si, Ca, and Ni abundances for IC 4756 (see Table 11) are also consistent those found by Luck (1994). He found [Si/H] = $+0.14 \pm 0.07$, [Ca/H] = -0.17 ± 0.11 , and [Ni/H] = $+0.05 \pm 0.07$, which agree with our values within the errors.

4.2. Iron in Open Clusters

The chemical evolution of the Milky Way has long been studied by identifying trends of element abundance with age or location in the Galaxy. In Figure 7 we plot [Fe/H] versus age and R_{gc} for the clusters in this study, along with results for other clusters that have been subject to high-resolution, detailed abundance analysis.

The lack of any trend of open cluster abundance with age is well established (see, e.g., Friel 1995; Salaris et al. 2004). The addition of our three data points to the sample does not change this. We note that systematics in any sample compiled from different sources may mask any real trend in the data, and stress the need for a large, homogeneous sample from which to base conclusions. Several groups are currently working on such samples, so it is only a matter of time before strong conclusions may be made. As noted by Yong et al. (2005), the lack of an abundance-age correlation could possibly be caused by clusters having different chemical enrichment histories. This has been noted in studies of thin- and thick-disk stars (see, e.g., Edvardsson et al. 1993; Reddy et al. 2003), and the recent work of Yong et al.

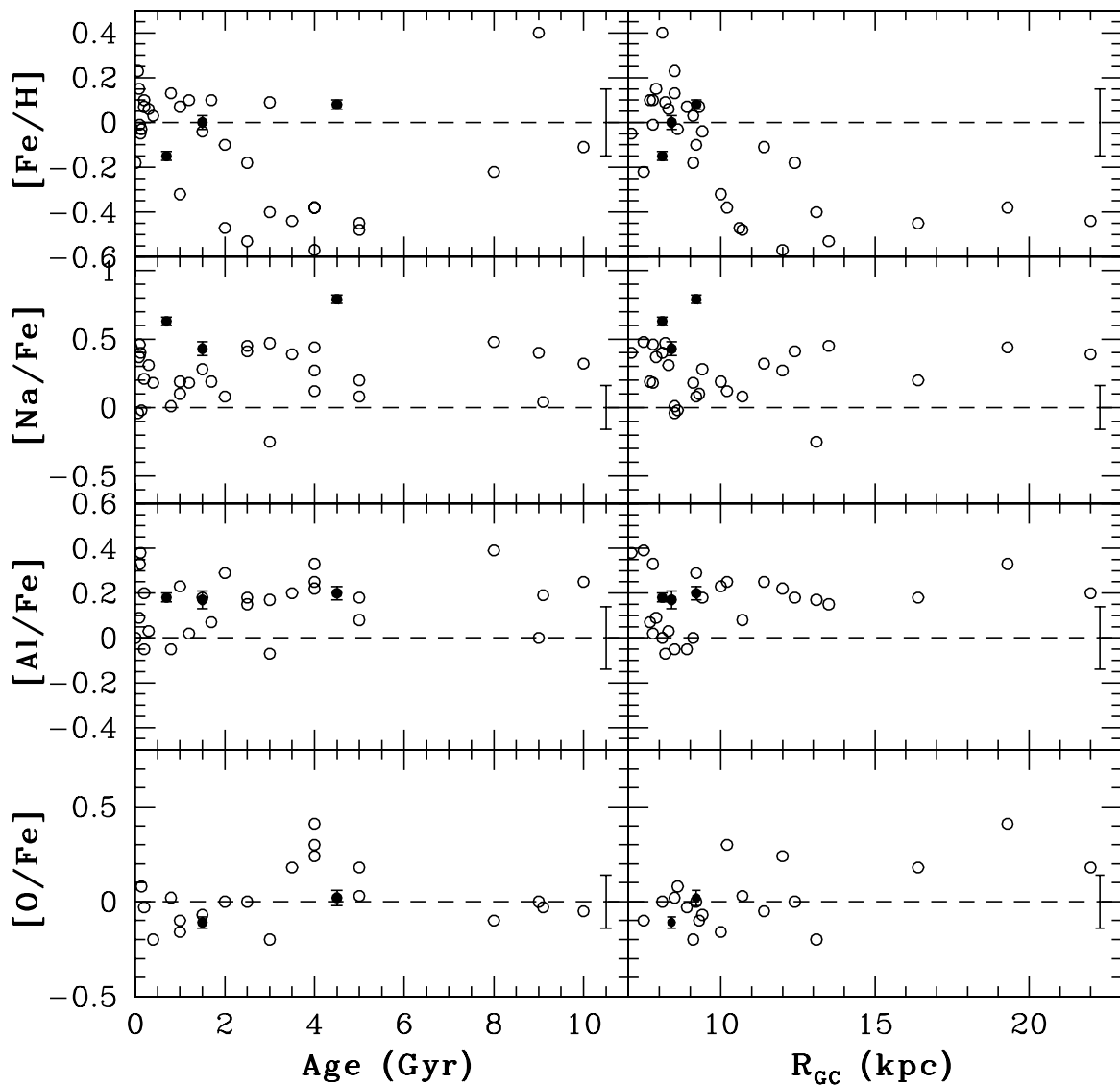


FIG. 7.—Fe, Na, Al, and O abundances for open clusters vs. R_{GC} and age. The error bars on the points indicate the standard error of the mean. The error bar located on the right of each plot represents the abundance uncertainty from Tables 12 and 13. Sources for the open cluster data include Bragaglia et al. (2001), Brown et al. (1996), Carraro et al. (2004), Cayrel et al. (1985), Edvardsson et al. (1995), Friel et al. (2003, 2005), Gonzalez & Wallerstein (2000), Gratton & Contarini (1994), Hamdani et al. (2000), Hill & Pasquini (1999), King et al. (2000), Luck (1994), Pasquini et al. (2004), Paulson et al. (2003), Peterson & Green (1998), Schuler et al. (2003, 2004), Smith & Suntzeff (1987), Tautvaisiene et al. (2000, 2005), Wilden et al. (2002), and Yong et al. (2005). [See the electronic edition of the Journal for a color version of this figure.]

(2005), among others, implies that outer disk clusters ($R_{GC} > 10$ –12 kpc) have indeed undergone a different enrichment history than those in the inner disk. That said, it is clear from the solar to supersolar metallicities of several of the older open clusters that at least some locations in the disk underwent chemical enrichment early on in the disk's formation.

A plot of Fe abundance versus galactocentric distance also yields clues to the enrichment history of the disk; we also show this in Figure 7. Much of the work on open cluster abundances has been motivated by the desire to precisely characterize the Fe abundance trend with location in the Galaxy. Clusters are only one of several tools in the astronomer's toolbox that have been used to probe this problem. Many studies of open clusters (e.g., Friel et al. 2002; Chen et al. 2003), B stars (e.g., Smartt & Rolleston 1997), planetary nebulae (e.g., Maciel et al. 2005), and H II regions (e.g., Rudolph et al. 2006) have used linear functions to characterize the abundance gradient. Twarog et al. (1997) characterized it as a step function, with the change in average open cluster abundance occurring around 10 kpc. The work of Yong

et al. (2005, 2006) and Carney et al. (2005) on clusters, red giants, and Cepheids, as well as the work of Andrievsky et al. (2002a, 2002b, 2002c, 2004) and Luck et al. (2003) on Cepheids, have supported Twarog et al.'s findings. Unfortunately, the clusters in our sample are all interior to the interesting 10 kpc region, and so cannot shed more light on the subject other than to reinforce the solar-like compositions found in the solar neighborhood. Indeed, examination of Figure 7 shows that IC 4756, NGC 6939, and NGC 7142 are well within the range of abundances for their locations in the disk.

4.3. Sodium and Aluminum in Open Clusters

4.3.1. NLTE Corrections

It is understood that abundances of light elements, particularly as determined from strong lines, may be prone to NLTE effects. In fact, some authors speculate that the overabundances of elements such as Na and Al seen in stars may be due to an inappropriate assumption of LTE, rather than real enhancements (Gratton et al.

1999). Unfortunately, such is the state of our understanding of NLTE effects, that not all workers choose to make NLTE corrections, and those that do often choose different corrections to make. This makes it especially difficult to compare results obtained by different authors for different clusters, and to choose how to address NLTE issues in this analysis.

Two papers in the literature present NLTE corrections for sodium abundances determined from several well-known and well-used absorption lines: Gratton et al. (1999) and Mashonkina et al. (2000). Unfortunately, as discussed by Johnson (2002), their results contradict one another. Considering only the Na doublet used in this analysis, Mashonkina et al. (2000) presented negative NLTE corrections that range from approximately -0.05 dex for dwarfs to -0.20 dex for cool giants. The Na line strengths calculated in their NLTE code are consistently stronger than LTE line strengths for model atmospheres of all temperatures and gravities they considered (see their Fig. 6). On the other hand, Gratton et al. (1999) stated that NLTE corrections for giants are for the most part *positive*, such that abundances derived in an LTE analysis underestimate the Na abundance by as much as 0.3 dex (see Fig. 15 in Gratton et al. 1999).

Because these two groups used different NLTE codes, treatment of the UV flux, etc., it should not be surprising that their results do not agree, but it is difficult to say which one should be preferred. Therefore, we opt not to perform any NLTE corrections for sodium.

We have not been able to find NLTE corrections for aluminum in the literature. Consequently, we present here LTE abundances for Al, and caution that NLTE corrections are likely to be necessary, and perhaps even large (~ 0.3 dex) in some cases. Gehren et al. (2004) report that NLTE corrections for aluminum are *positive*, in which case, they would only increase the Al enhancements seen in these stars.

We stress that the abundance patterns of these elements cannot really be explored until it is known how to deal with NLTE effects correctly. At minimum, this requires agreement among different groups as to which direction the corrections go.

4.3.2. Na and Al in Open Clusters

Whatever NLTE correction one chooses, Na abundances are enhanced in all three clusters (see Table 9). Plots of $[\text{Na}/\text{Fe}]$ (synthesis analysis) and $[\text{Al}/\text{Fe}]$ (synthesis analysis) versus age and R_{gc} are included in Figure 7. When comparing the $[\text{Na}/\text{Fe}]$ abundances of NGC 7142, NGC 6939, and IC 4756 to those of other clusters, it is important to keep in mind the 0.2–0.3 dex difference between our Arcturus-derived $\log gf$ values and the solar- or laboratory-measured $\log gf$ values that are used by most other studies. Note that four other clusters in Figure 7 use our Arcturus-derived $\log gf$ values: Cr 261 (Friel et al. 2003), Be 17 (Friel et al. 2005), Be 29, and Saurer 1 (Carraro et al. 2004). Using solar gf -values would decrease $[\text{Na}/\text{Fe}]$ in our analysis by ~ 0.2 dex, which is more consistent with the enhancements found by studies of other open clusters as seen in Figure 7.

Such enhancements of Na in giants may be due to dredge-up (see, e.g., Pasquini et al. 2004). Extra sodium is produced in the NeNa cycle, which is thought to occur during shell burning. If Na enhancements are attributable to dredge-up, it can be supposed that $[\text{Na}/\text{Fe}]$ values would show some dependence on $\log g$ (Mishenina et al. 2006). We plotted EW $[\text{Na}/\text{Fe}]$ values versus $\log g$ for all three clusters. There is a large amount of scatter; the relative contributions of measurement errors, errors in atmospheric parameters, intrinsic star-to-star variations, and NLTE issues are impossible to disentangle. No trend of abundance with gravity was discernible. In case possible errors in the gravity

calculations for the stars were masking any trends, we also plotted $[\text{Na}/\text{Fe}]$ versus V magnitude and again saw no clear trend.

Evolved stars in globular clusters can have a strong Na-O abundance anticorrelation (see, e.g., Fig. 16 of Ivans et al. 2001). While this anticorrelation may be evidence of the ON and NeNa cycles occurring in these stars, recent studies have found the Na-O anticorrelation in unevolved stars of certain globular clusters as well, implying a primordial origin (Gratton et al. 2001). A similar anticorrelation has yet to be found in any open cluster stars (Carretta et al. 2005). Plots of $[\text{Na}/\text{H}]$ versus $[\text{O}/\text{H}]$ for stars in NGC 7142 and NGC 6939 show no evidence of an anticorrelation.

As discussed previously, aluminum enhancements in our clusters are smaller than those of sodium; such is the case for open clusters in general, as seen in Figure 7. IC 4756, NGC 6939, and NGC 7142 exhibit the same range of $[\text{Al}/\text{Fe}]$ for open clusters as a function of both age and galactocentric distance.

4.4. Oxygen

Oxygen abundance is a useful tracer of chemical enrichment, particularly when compared to Fe; $[\text{O}/\text{Fe}]$ is plotted against age and R_{gc} in Figure 7. While no clear trend with age is visible, the distribution of $[\text{O}/\text{Fe}]$ is markedly different for inner and outer disk clusters, as mentioned by Yong et al. (2005). This is a strong indication that the inner disk and outer disk have undergone different enrichment histories. NGC 6939 and NGC 7142 have $[\text{O}/\text{Fe}]$ values consistent with their location in the inner disk.

We refer the reader to Figure 23 of Yong et al. (2005), which plots $[\text{O}/\text{Fe}]$ versus $[\text{Fe}/\text{H}]$ for open clusters, thin-disk stars, and thick-disk stars. The majority of stars with high $[\text{O}/\text{Fe}]$ and low $[\text{Fe}/\text{H}]$ values are thick-disk stars. While some open clusters have $[\text{O}/\text{Fe}]$ within the lower range of values for thick-disk stars, the majority have values that are consistent with thin-disk stars, as is the case for NGC 7142 and NGC 6939.

4.5. Si, Ca, and Ni

As seen in Table 10, the dispersion about the mean abundance for Si, Ca, and Ni for individual stars is large, and increases with increasing abundance, most notably for Si and for the NGC 7142 stars. However, the star-to-star variation in each cluster shown by the cluster mean and standard deviation (Table 11) is relatively small (~ 0.1 dex). A few stars do deviate from the mean. Star 292 in NGC 6939 has much larger Ca and Ni abundances than the other cluster members; recall that its atmospheric parameters are less certain. Also in NGC 6939, stars 31 and 212 have larger Si abundances than the other stars. The atmospheric parameters of 212 also have less certainty, while 31 is the coolest star in the entire sample. If one excludes 292, the standard deviation of the mean Ca abundance for NGC 6939 decreases to 0.06 dex.

Figure 8 shows $[\text{Si}/\text{Fe}]$ and $[\text{Ca}/\text{Fe}]$ plotted against age and galactocentric distance. While it is clear that the abundances of the three clusters fall within the range of values for their age and location, all show large enhancements of Si, especially NGC 7142. Five of the six stars in NGC 7142 have $[\text{Si}/\text{Fe}] = +0.32$ or greater, and unlike for NGC 6939, the star in the sample with more uncertain atmospheric parameters (229) does not show the largest enhancements. At the resolution of our data, the $\text{Si I } \lambda 6243.8$ line is badly blended. $\text{Si I } \lambda 6145.0$ is also blended with a line of comparable strength just redward of it, while the wing of $\text{Si I } \lambda 6142.5$ is slightly blended with a much stronger line just blueward of it. The abundance of one of these lines invariably differs greatly from the other two for each star in the sample, but both the culprit line and the “direction” of the deviation vary from star to star. Therefore, all we can say is that the high Si abundance in

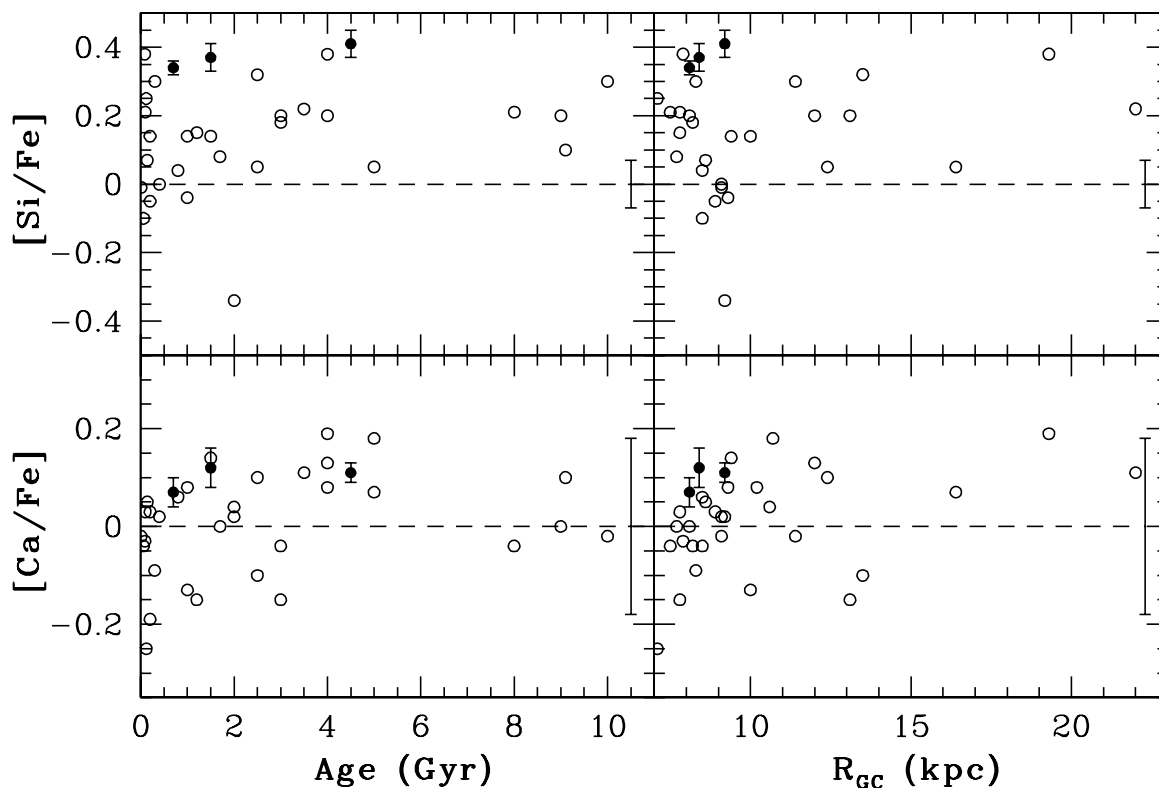


FIG. 8.—Si and Ca abundances for open clusters vs. R_{GC} and age. Error bars on the points indicate the standard error of the mean. The error bar located on the right of each plot represents the abundance uncertainty from Table 12. See Fig. 7 for references. [See the electronic edition of the Journal for a color version of this figure.]

NGC 7142 is likely in part caused by blending of the Si features with other strong lines that were not properly accounted for in the EW measuring process. That said, it is also worth noting that $[Si/Fe]$ is high in many other clusters (Fig. 8). The average Ca abundances for the three clusters are more consistent with other clusters in the inner disk. As expected, abundances of the iron-peak element Ni roughly scale with Fe, within the errors.

4.6. Lithium Abundances in NGC 6939

Stars 31, 121, and 212 in NGC 6939 show strong Li $\lambda 6707.7$ features (see Fig. 9). Lithium abundances for these stars were

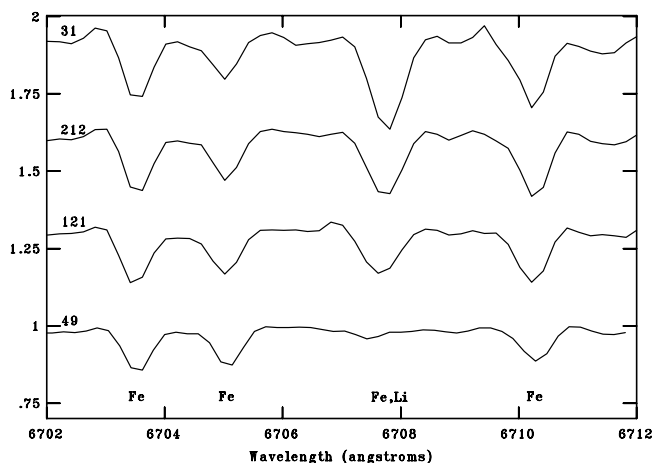


FIG. 9.—Spectral region around the Li $\lambda 6707.7$ feature in NGC 6939 stars 121 (lower middle), 212 (upper middle), and 31 (top). IC 4756 star 49 is shown at the bottom for comparison. The NGC 6939 stars have been corrected for radial velocity shifts.

determined by spectrum synthesis. The synthesis line list was taken from Reddy et al. (2002), although here we assume that only ${}^7\text{Li}$ is present. The method of analysis has been described in earlier sections. We found the lithium abundances of stars 31, 121, and 212 to be $\log N(\text{Li}) = 0.8, 1.0,$ and 1.1 , respectively. Due to the blending of the Li feature with other lines, and the quality of the synthesis fits, the likely uncertainty of these measurements is ~ 0.15 dex.

Lithium-rich stars are commonly identified in the literature as having $\log N(\text{Li}) > 1.4$ (Charbonnel & Balachandran 2000; Reddy & Lambert 2005). None of these stars is lithium-rich; in fact, studies of other open clusters imply that their lithium abundances are normal. Pilachowski (1986) presented a study of Li abundances in evolved stars in open cluster NGC 7789, whose age, metallicity, and CMD morphology are similar to those of NGC 6939. Pilachowski (1986) divided her sample into six groups based on evolutionary state and found that the Li abundances decreased with advanced evolutionary state. This is consistent with Li being destroyed at the base of the convection zone in these stars, in agreement with modern theoretical predictions (Charbonnel & Balachandran 2000). Stars 31, 121, and 212, in their position above the clump in the CMD (Fig. 2), are analogous to the group III giants in Pilachowski (1986, see Fig. 1) and indeed have comparable Li abundances.

We offer a caveat to our Li abundances. Gilroy (1989) and Luck (1994) measured the Li abundances of stars in IC 4756. Gilroy (1989) determined $\log N(\text{Li}) = 0.55, 0.30, 0.45, 0.30,$ and 0.40 for stars 49, 69, 101, 109, and 125, respectively. Luck (1994) found $\log N(\text{Li}) = 0.69$ for star 49, which is also shown in Figure 9. We analyzed the stars we have in common with Gilroy and Luck and could not reproduce their results, instead getting $\log N(\text{Li}) < 0$. If our synthesis of this region is in error, the Li abundances of these NGC 6939 stars may be much larger than

reported here. These stars should be examined at higher spectral resolution; C and N isotopic abundances would also be useful.

5. SUMMARY

We have carried out a detailed abundance analysis of six to nine stars in each of the open clusters NGC 7142, NGC 6939, and IC 4756. Abundances of the elements Fe, Na, Al, O, Si, Ca, and Ni were determined via equivalent width and spectrum synthesis analysis. The iron abundances of NGC 7142, NGC 6939, and IC 4756 ($[Fe/H] = +0.08 \pm 0.06, +0.00 \pm 0.10, \text{ and } -0.15 \pm 0.04$, respectively) are consistent both with values found by previous studies and with the range of $[Fe/H]$ shown by other open clusters at their galactocentric distances.

All three clusters show large Na enhancements of order 0.4–0.6 dex, while $[Al/Fe]$ is ~ 0.1 –0.2 dex. While NLTE corrections might decrease the Na enhancements, it is unlikely that they will disappear in all three clusters. Star-to-star dispersion within the clusters is small. As the number of open clusters showing these enhancements increases, it is necessary to resolve the ambiguity of Na NLTE corrections that currently exists in the literature. Average abundances of Ca, Si, and Ni for these clusters are also consistent with those of other clusters at their galactocentric dis-

tances, with $[Si/Fe]$ being enhanced. As for oxygen, $[O/Fe]$ values for NGC 7142 and NGC 6939 are consistent with their location in the inner disk. Finally, we have discovered three stars in NGC 6939 with large lithium abundances: $\log N(Li) \sim 1.0$.

H. R. J. thanks the WIYN 3.5 m telescope operators for their invaluable assistance and Bertrand Plez for kindly providing the CN line list. C. A. P. gratefully acknowledges the support of the Daniel Kirkwood Research Fund at Indiana University. We also thank the referee, Bruce A. Twarog, for his helpful suggestions and comments that improved the quality of this paper. This research is supported by a National Science Foundation Graduate Research Fellowship. This publication makes use of data products from the Two Micron All Sky Survey, which is a joint project of the University of Massachusetts and the Infrared Processing and Analysis Center/California Institute of Technology, funded by the National Aeronautics and Space Administration and the National Science Foundation. This study also uses the WEBDA database, operated at the Institute for Astronomy of the University of Vienna, and the Vienna Atomic Line Database.

REFERENCES

- Alcaino, G. 1965, *Lowell Obs. Bull.*, 6, 167
- Alonso, A., Arribas, S., & Martinez-Roger, C. 1999, *A&AS*, 140, 261
- Andruzzi, G., Bragaglia, A., Tosi, M., & Marconi, G. 2004, *MNRAS*, 348, 297 (A04)
- Andrievsky, S. M., Bersier, D., Kovtyukh, V. V., Luck, R. E., Maciel, W. J., Lepine, J. R. D., & Beletsky, Y. V. 2002a, *A&A*, 384, 140
- Andrievsky, S. M., Kovtyukh, V. V., Luck, R. E., Lepine, J. R. D., Maciel, W. J., & Beletsky, Y. V. 2002b, *A&A*, 392, 491
- Andrievsky, S. M., Luck, R. E., Martin, P., & Lepine, J. R. D. 2004, *A&A*, 413, 159
- Andrievsky, S. M., et al. 2002c, *A&A*, 381, 32
- Bell, R., Eriksson, K., Gustafsson, B., & Nordlund, Å. 1976, *A&AS*, 23, 37
- Bragaglia, A., et al. 2001, *AJ*, 121, 327
- Brown, J. A., Wallerstein, G., Geisler, D., & Oke, J. B. 1996, *AJ*, 112, 1551
- Cannon, R. D., & Lloyd, C. 1969, *MNRAS*, 144, 449
- Cannon, R. D., & Purcell, A. G. 1970, *R. Obs. Bull.*, 158, 69
- Canterna, R., Geisler, D., Harris, H. C., Olszewski, E., & Schommer, R. 1986, *AJ*, 92, 79
- Camey, B. W., Yong, D., Teixeira de Almeida, M. L., & Seitzer, P. 2005, *AJ*, 130, 1111
- Carraro, G., Bresolin, F., Villanova, S., Matteucci, F., Patat, F., & Romaniello, M. 2004, *AJ*, 128, 1676
- Carretta, E., Bragaglia, A., Gratton, R. G., & Tosi, M. 2005, *A&A*, 441, 131
- Cayrel, R., Cayrel de Strobel, G., & Campbell, B. 1985, *A&A*, 146, 249
- Charbonnel, C., & Balachandran, S. C. 2000, *A&A*, 359, 563
- Chen, L., Hou, J. L., & Wang, J. J. 2003, *AJ*, 125, 1397
- Chincari, G. 1963, *Contr. Asiago*, 138
- Crinklaw, G., & Talbert, F. D. 1991, *PASP*, 103, 536 (CT91)
- Cutri, R. M., et al. 2003, *The IRSA 2MASS All-Sky Point Source Catalog (Pasadena: NASA/IPAC)*
- Di Benedetto, G. P. 1998, *A&A*, 339, 858
- Edvardsson, B., Andersen, J., Gustafsson, B., Lambert, D. L., Nissen, P. E., & Tomkin, J. 1993, *A&A*, 275, 101
- Edvardsson, B., Pettersson, B., Kharrazi, M., & Westerlund, B. 1995, *A&A*, 293, 75
- El Eid, M. F., & Champagne, A. E. 1995, *ApJ*, 451, 298
- Friel, E. D. 1995, *ARA&A*, 33, 381
- Friel, E. D., Jacobson, H. R., Barrett, E., Fullton, L., Balachandran, S., & Pilachowski, C. A. 2003, *AJ*, 126, 2372
- Friel, E. D., Jacobson, H. R., & Pilachowski, C. A. 2005, *AJ*, 129, 2725
- Friel, E. D., & Janes, K. A. 1993, *A&A*, 267, 75
- Friel, E. D., Janes, K. A., Tavaréz, M., Scott, J. E., Katsanis, R., Lotz, J., Hong, L., & Miller, N. 2002, *AJ*, 124, 2693
- Friel, E. D., Liu, T., & Janes, K. A. 1989, *PASP*, 101, 1105
- Fulbright, J. P., McWilliam, A., & Rich, R. M. 2006, *ApJ*, 636, 821
- Gehren, T., Liang, Y. C., Shi, J. R., Zhang, H. W., & Zhao, G. 2004, *A&A*, 413, 1045
- Gilroy, K. K. 1989, *ApJ*, 347, 835
- Glushkova, E. V., & Rastorguev, A. S. 1991, *Soviet Astron. Lett.*, 17, 64
- Gonzalez, G., & Wallerstein, G. 2000, *PASP*, 112, 1081
- Gratton, R., Carretta, E., Eriksson, K., & Gustafsson, B. 1999, *A&A*, 350, 955
- Gratton, R., & Contarini, G. 1994, *A&A*, 283, 911
- Gratton, R., et al. 2001, *A&A*, 369, 87
- Hamdani, S., North, P., Mowlavi, N., Raboud, D., & Mermilliod, J.-C. 2000, *A&A*, 360, 509
- Herzog, A. D., Sanders, W. L., & Seggewiss, W. 1975, *A&AS*, 19, 211
- Hoag, A. A., Johnson, H. L., Iriarte, B., Mitchell, R. I., Hallam, K. L., & Sharpless, S. 1961, *Publ. US Naval Obs.*, 17, 345
- Hill, V., & Pasquini, L. 1999, *A&A*, 348, L21
- Hill, V., et al. 2002, *A&A*, 387, 560
- Hinkle, K., Wallace, L., Valenti, J., & Harmer, D. 2000, *Visible and Near Infrared Atlas of the Arcturus Spectrum (San Francisco: ASP)*
- Ivans, I. I., Kraft, R. P., Sneden, C., Smith, G. H., Rich, R. M., & Shetrone, M. 2001, *AJ*, 122, 1438
- Jennens, P. A., & Helfer, H. L. 1975, *MNRAS*, 172, 681
- Johnson, J. A. 2002, *ApJS*, 139, 219
- King, J. R., Soderblom, D. R., Fischer, D., & Jones, B. F. 2000, *ApJ*, 533, 944
- Kopff, E. 1943, *Astron. Nachr.*, 274, 69
- Kupka, F., Ryabchikova, T. A., Piskunov, N. E., Stempels, H. C., & Weiss, W. W. 2000, *Baltic Astron.*, 9, 590
- Kustner, F. 1923, *Veroeffentlichungen Univ.-Sternw. Bonn*, 18, 1
- Luck, R. E. 1994, *ApJS*, 91, 309
- Luck, R. E., Gieren, W. P., Andrievsky, S. M., Kovtyukh, V. V., Fouque, P., Pont, F., & Kienzle, F. 2003, *A&A*, 401, 939
- Lynga, G., & Lundstrom, I. 1980, in *IAU Symp. 85, Star Clusters*, ed. J. E. Hesser (Dordrecht: Reidel), 123
- Maciel, W. J., Lago, L. G., & Costa, R. D. D. 2005, *A&A*, 433, 127
- Mashonkina, L. I., Shimanskii, V. V., & Sakhbullin, N. A. 2000, *Astron. Rep.*, 44, 790
- Mermilliod, J.-C., Huestamendia, G., & del Rio, G. 1994, *A&AS*, 106, 419
- Mermilliod, J.-C., & Mayor, M. 1990, *A&A*, 237, 61 (MM90)
- Meurers, J., & Scharf, K. J. 1957, *Veroeffentlichungen Univ.-Sternw. Bonn*, 48, 1
- Milone, A. A. E. 1994, *PASP*, 106, 1085
- Mishenina, T. V., Bienayme, O., Gorbaneva, T. I., Charbonnel, C., Soubiran, C., Korotin, S. A., & Kovtyukh, V. V. 2006, *A&A*, 456, 1109
- Pasquini, L., Randich, S., Zoccali, M., Hill, V., Charbonnel, C., & Nordstrom, B. 2004, *A&A*, 424, 951
- Paulson, D. B., Sneden, C., & Cochran, W. D. 2003, *AJ*, 125, 3185
- Pendl, E. S., & Seggewiss, W. 1975, in *IAU Coll. 32, Physics of Ap Stars*, ed. W. W. Weiss, H. Jenkner, & J. H. Wood (Wien: Univ. Wien), 357
- Peterson, R. C., Dalle Ore, C. M., & Kurucz, R. L. 1993, *ApJ*, 404, 333
- Peterson, R. C., & Green, E. M. 1998, *ApJ*, 502, L39
- Pilachowski, C. A. 1986, *ApJ*, 300, 289
- Randich, S., Sestito, P., Primas, F., Pallavicini, R., & Pasquini, L. 2006, *A&A*, 450, 557
- Reddy, B. E., & Lambert, D. L. 2005, *AJ*, 129, 2831

- Reddy, B. E., Lambert, D. L., Laws, C., Gonzalez, G., & Covey, K. 2002, MNRAS, 335, 1005
- Reddy, B. E., Tomkin, J., Lambert, D. L., & Allende Prieto, C. 2003, MNRAS, 340, 304
- Risley, A. M. 1943, ApJ, 97, 277
- Rosvick, J. M., & Balam, D. 2002, AJ, 124, 2093 (RB02)
- Rudolph, A. L., Fich, M., Bell, G. R., Norsen, T., Simpson, J. P., Haas, M. R., & Erickson, E. F. 2006, ApJS, 162, 346
- Salaris, M., Weiss, A., & Percival, S. M. 2004, A&A, 414, 163
- Schmidt, E. G. 1978, PASP, 90, 157
- Schuler, S. C., King, J. R., Fischer, D. A., Soderblom, D. R., & Jones, B. F. 2003, AJ, 125, 2085
- Schuler, S. C., King, J. R., Hobbs, L. M., & Pinsonneault, M. H. 2004, ApJ, 602, L117
- Sestito, P., Randich, S., & Bragaglia, A. 2007, A&A, 465, 185
- Sharov, A. S. 1965, Soviet Astron., 8, 780
- Smartt, S. J., & Rolleston, W. R. J. 1997, ApJ, 481, L47
- Smith, G. E. 1983, PASP, 95, 296
- Smith, V. V., & Suntzeff, N. B. 1987, AJ, 93, 359
- Snedden, C. 1973, Ph.D. thesis, Univ. Texas, Austin
- Tautvaisiene, G., Edvardsson, B., Puzeras, E., & Ilyin, I. 2005, A&A, 431, 933
- Tautvaisiene, G., Edvardsson, B., Touminen, I., & Ilyin, I. 2000, A&A, 360, 499
- Thogersen, E. N., Friel, E. D., & Fallon, B. V. 1993, PASP, 105, 1253
- Twarog, B. A., Ashman, K. M., & Anthony-Twarog, B. J. 1997, AJ, 114, 2556
- VandenBerg, D. A. 1985, ApJS, 58, 711
- van den Bergh, S. 1962, J. R. Astron. Soc. Canada, 56, 41
- van den Bergh, S., & Heeringa, R. 1970, A&A, 9, 209
- Wilden, B. S., Jones, B. F., Lin, D. N. C., & Soderblom, D. R. 2002, AJ, 124, 2799
- Yong, D., Carney, B. W., & Teixeira de Almeida, M. L. 2005, AJ, 130, 597
- Yong, D., Carney, B. W., Teixeira de Almeida, M. L., & Pohl, B. L. 2006, AJ, 131, 2256